

Accepted Manuscript

Kinetics and synthesis of low molecular weight polyesters from ϵ -caprolactone and L-lactide catalyzed by Zn(II) and Cu(II) N-Hydroxy *N,N'*-diarylformamidine complexes

Wisdom A. Munzeiwa, Bernard Omondi, Vincent O. Nyamori

PII: S0277-5387(17)30606-X

DOI: <https://doi.org/10.1016/j.poly.2017.09.029>

Reference: POLY 12839

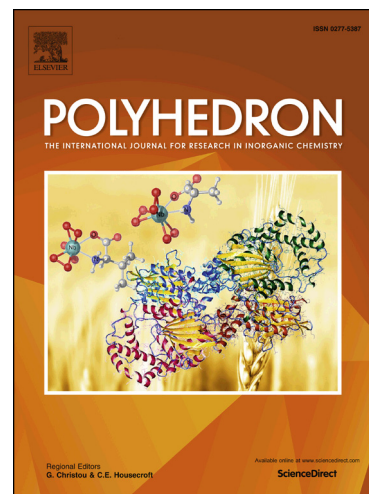
To appear in: *Polyhedron*

Received Date: 1 July 2017

Accepted Date: 17 September 2017

Please cite this article as: W.A. Munzeiwa, B. Omondi, V.O. Nyamori, Kinetics and synthesis of low molecular weight polyesters from ϵ -caprolactone and L-lactide catalyzed by Zn(II) and Cu(II) N-Hydroxy *N,N'*-diarylformamidine complexes, *Polyhedron* (2017), doi: <https://doi.org/10.1016/j.poly.2017.09.029>

This is a PDF file of an unedited manuscript that has been accepted for publication. As a service to our customers we are providing this early version of the manuscript. The manuscript will undergo copyediting, typesetting, and review of the resulting proof before it is published in its final form. Please note that during the production process errors may be discovered which could affect the content, and all legal disclaimers that apply to the journal pertain.



Kinetics and synthesis of low molecular weight polyesters from ϵ -caprolactone and L-lactide catalyzed by Zn(II) and Cu(II) N-Hydroxy *N,N'*-diarylformamidine complexes

Wisdom A. Munzeiwa, Bernard Omondi* and Vincent O. Nyamori

School of Chemistry and Physics, University of KwaZulu-Natal, Westville Campus, Private Bag X54001, Durban 4000, South Africa

*E-mails: owaga@ukzn.ac.za

ABSTRACT

Discrete Zn(II) and Cu(II) complexes have been synthesized using *N*-hydroxy-*N,N'*-diarylformamidine ligands: *N*-hydroxy-*N,N'*-bis(2,6-diisopropylphenyl)formamidine (**L1**), *N*-hydroxy-*N,N'*-bis(2,6-dimethyl)formamidine (**L2**), *N*-hydroxy-*N*-(2-methoxyphenyl)-*N'*-(2,6-diisopropylphenyl)formamidine (**L3**), and *N*-hydroxy-*N*-(2-methoxyphenyl)-*N'*-(2,6-dimethylphenyl)formamidine (**L4**). Reaction of ligands **L1** - **L4** with either ZnOAc₂·2H₂O or CuOAc₂·2H₂O in aqueous ethanol gave mononuclear complexes [Zn-(**L1**)₂] (**1**), Zn-(**L2**)₂] (**2**), Zn-(**L3**)₂] (**3**), [Zn-(**L4**)₂] (**4**), and [Cu-(**L1**)₂] (**5**), [Cu-(**L2**)₂] (**6**), [Cu-(**L3**)₂] (**7**), [Cu-(**L4**)₂] (**8**), as Zn(II) and Cu(II) complexes, respectively, with high yields of up to 84%. All the complexes were characterized by elemental analysis, IR, NMR and mass spectroscopies. The molecular structures of complexes **3** and **7** were determined by single crystal X-ray diffraction analyses. The Zn(II) center in complex **3** exhibited a distorted tetrahedral geometry while in complex **7**, the Cu(II) center had a square planar geometry with near *C*₂ symmetry. In both structures, the coordination sites are occupied by imino *N* and hydroxyl *O* donor atoms from the chelating ligands. All complexes showed catalytic activity in ring-opening polymerization of ϵ -caprolactone and L-lactide in the presence of a co-initiator and exhibited well-controlled living polymerization process. The molecular weights were found to be low ranging from 1855 - 3999 Da for polycaprolactone (PCL) and up to 1720 Da for polylactic acid (PLA). The Zn(II) catalysts were found to be more active than Cu(II) catalysts with complex **2** ($k_{app} = 0.1751 \text{ h}^{-1}$) being the most active.

Keywords:

Zn(II), Cu(II), polyesters, ROP, kinetics, *N*-Hydroxy-*N,N'*-diarylformamidine

1.0 Introduction

Petroleum based-polymers that are derived from nonrenewable fossils have low biodegradability and cause environmental pollution after disposal [1]. In addressing these challenges, modern-day polymer research is geared towards developing economically viable, recyclable and biodegradable polymers derived from renewable resources. Aliphatic polyesters have emerged as better surrogates and they present many traits. Poly(lactic acid) (PLAs) and poly(ϵ -caprolactone) (PCLs) are interesting candidates because they are bio-compatible, bio-degradable and can be bio-derived. Owing to their diverse applications in the field of medicine [2], packaging [3] and electronic devices [4], their demand has increased over the past decades. Metal-based ring opening polymerization (ROP) has indisputably proved to be a more proficient method for the synthesis of polyesters.

Commercially, tin(II) complexes are used as catalyst or initiators for the synthesis of PCLs and PLAs, however their toxicities limits their use in the production of polymers for medical applications since the elimination of remnant catalyst from the polymer is a challenge [5]. Coordination complexes of cheap and bio-compatible metals with reasonable toxicity are now being investigated as replacements. Metals such as zinc [6], magnesium [7], calcium [8], aluminum [9] and copper [10] have been investigated and have shown promising results towards ROP of cyclic esters. Alkali earth metals [11] and lanthanides [12] have also been explored for catalytic activity in ROP. More recently, silver which is known to have antimicrobial properties have been found to be active towards ϵ -caprolactone (ϵ -CL) polymerization [13].

A metal-oxygen bond is a prerequisite for effective initiation of the polymerization process. Many metal-based ROP systems are dominated by nitrogen and/or oxygen as metal stabilizing ligands which have a positive influence towards catalytic activity [15]. Ligand-supported single site metal alkoxide initiators have been shown to control the polymerization process and yield polymers with controlled molecular weights (M_w), polydispersity indices (PDIs), architecture and end groups [14]. This has attracted much interest and prompted researchers to design more ligands to support metal-alkoxide based catalyst for ROP. Salen-type ligand supported metal initiators have been systematically studied and used effectively in ROP of lactides with high stereo-control toward, either isotactic or heterotactic PLA polymers [16].

Apart from the chemical properties, physical properties of auxiliary ligands also impact strongly on the catalytic activity of metal based catalyst. Thus, it is paramount to probe correlation between ligand structure and catalytic activity. From previous work reported by our group, *N,N'*-diarylformamidines ligands have been used to support Zn(II) and Cu(II) complexes which were active in ROP ϵ -CL and L-LA. Herein, the *N,N'*-diarylformamidines ligands were modified to *N*-hydroxy-*N,N'*-diarylformamidines ligands which potentially introduce M—O bonds as part of the catalyst. We hypothesized that the presence of M—O bonds will bring enhanced catalytic activity as well as polymer characteristics.

2.0 Experimental section

2.1 Materials

All experiments were carried out under argon, 5.0 technical grade, (Airflex Industrial Gases, South Africa) using Schlenk techniques. All solvents were obtained from Sigma-Aldrich. Reagent grade absolute ethanol (98%) was distilled and dried from magnesium turnings; dichloromethane (DCM), (99%) and hexane (98%) were dried from sodium–benzophenone mixture. Reagents, Cu(OAc)₂·H₂O (98%), Zn(OAc)₂·2H₂O (97%), ϵ -caprolactone (ϵ -CL) (98%) and L-lactide (L-LA) 97% and 3-chloroperoxybenzoic acid, (MCPBA) (77%) were obtained from Sigma-Aldrich. Anhydrous MgSO₄ (98%), NaOH (99%), anhydrous NaHCO₃ (97%) and anhydrous K₂CO₃ (99%) were obtained from Promark Chemicals, South Africa.

2.2 Instrumentation

¹H and ¹³C NMR spectra were measured at room temperature on a Bruker Avance^{III} 400MHz spectrometer. Both ¹H NMR and ¹³C NMR data was recorded in CDCl₃ and referenced to the residual CDCl₃ peaks at δ 7.26 and δ 77.00, respectively. IR spectra were obtained on a PerkinElmer Universal ATR spectrum 100 FTIR spectrometer. Mass spectra of complexes were obtained from a Water synapt GR electrospray positive spectrometer.

3.0 General synthesis methods

3.1 Synthesis of *N*-hydroxy *N,N'* diarylformamidine ligands

Amidine (1.0 mmol) was dissolved in DCM and solid sodium hydrogen carbonate (1.0 mmol) was then added and the mixture cooled to 0 °C. Thereafter, *m*-MCPBA (1.2 mmol) in DCM was added dropwise and the reaction mixture was allowed to warm to room temperature with stirring for a further 1 h. The reaction mixture was then washed with a solution of potassium carbonate (5%; 2 × 25 ml) and the combined organic fractions were dried over anhydrous sodium sulphate and filtered. The solvent was then removed by evaporation to afford, *N*-hydroxy-*N,N'*-bis(2,6-diisopropylphenyl)formamidine (**L1**), *N*-hydroxy-*N,N'*-bis(2,6-dimethyl)formamidine (**L2**), and *N*-hydroxy-*N*-(2-methoxyphenyl)-*N'*-(2,6 dimethylphenyl)formamidine (**L4**) as solids whilst *N*-hydroxy-*N*-(2-methoxyphenyl)-*N'*-(2,6-diisopropylphenyl)formamidine (**L3**), was obtained an oil (Fig.1).

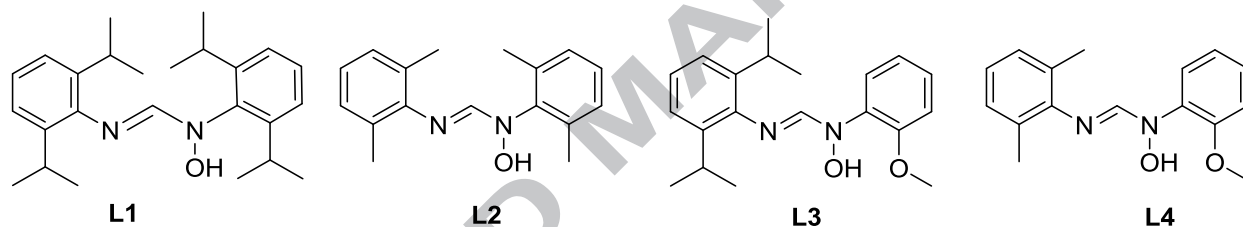


Fig. 1. *N*-hydroxy-*N,N'*-diarylformamidine ligands employed in the synthesis of complexes reported herein

3.2 Synthesis of Zn(II) and Cu(II) complexes

The respective hydrated metal acetate salt (1 mmol) was dissolved in water and the pH adjusted to 8.0 using 1M NaOH solution. Thereafter, a solution of the ligand (2.0 mmol) in aqueous ethanol 90% was added. A precipitate was formed immediately in each case and the reaction mixture was stirred at room temperature for 8 h. Deionized water (100 ml) was added and then the temperature lowered to 4 °C and the mixture stirred for a further 2 h. The resultant solids were collected by filtration, washed with hot water and aqueous ethanol (50%). The complexes were then dissolved in DCM, dried with anhydrous MgSO₄, filtered and by slow evaporation of the solvent, the desired products were obtained as solids (see Scheme 2).

3.2.1 [Zn-(L1)₂] (1)

The reaction of **L1** (0.30 g, 0.788 mmol) and Zn(OAc)₂·2H₂O (0.076 g, 0.394 mmol) in ethanol furnished complex **1** as a white powder. Yield 86%. Melting point 187 – 189 °C. ¹H NMR (CDCl₃, 400 MHz): δ (ppm) 0.79 (d, ³J_{H,H} = 6.84, 12H, ⁱPr-CH₃), 1.09 (dd, ³J_{H,H} = 6.80 Hz, 12H, ⁱPr-CH₃), 1.20 (d, ³J_{H,H} = 6.88 Hz, 12H, ⁱPr-CH₃), 1.35 (d, ³J_{H,H} = 6.72 Hz, 12H, ⁱPr-CH₃), 3.24 (qn, ³J_{H,H} = 4.80, 8H, CH ⁱPr-CH_{methine}), 7.02 (q, ³J_{H,H} = 1.96 Hz, 4H, Ar), 7.19 (s, 2H, Ar), 7.11 - 7.15 (m, 2H, Ar), 7.20 (s, NC(H)N), 7.33 (t, ³J_{HH} = 7.78 Hz, 2H, Ar). ¹³C NMR (CDCl₃, 400 MHz): δ (ppm) 23.6, 23.9, 24.2, 24.6, 25.5, 27.8, 28.3, 123.2, 124, 129.8, 137.6, 142.5, 143.2, 145.8, 147.5, 150.0. IR: ν (cm⁻¹) 2961 (s), 2868 (w), 1663 (s), 1607 (s), 1441 (m), 1288 (w). ESI-TOF MS: m/z (%) 845.6 (100) [M + Na]⁺. Elemental analysis calcd (%) for C₅₀H₇₀N₄O₂Zn: C, 72.83; H, 8.56; N, 6.80. Found: C, 72.70; H, 8.18; N, 6.87.

3.2.2 [Zn-(L2)₂] (2)

The reaction of ligand **L2** (0.30 g, 0.788 mmol) and Zn(OAc)₂·2H₂O (0.076 g, 0.394 mmol) in ethanol furnished complex **2** as a white powder. Yield 74%. Melting point: 242- 245 °C. ¹H NMR (CDCl₃, 400 MHz): δ (ppm) 2.04 (s, 12H, CH₃), 2.29 (s, 12H, CH₃) 6.95 - 6.92 (m, ³J_{H,H} = 4.91 Hz, 4H, Ar), 7.01 (d, ³J_{H,H} = 7.4 Hz 4H, Ar), 7.07 (d, ³J_{H,H} = 7.56 Hz, 4H, Ar), 7.31 (s, 2H, NCHN). ¹³C NMR (CDCl₃, 400 MHz): δ (ppm) 17.4, 18.5, 124.2, 128, 128.3, 129, 132.7, 136.8, 139.8, 144.8, 148.8. IR: ν (cm⁻¹) 2964(w), 1610(s), 1598(s), 1471(w), 1206(s). ESI-TOF MS: m/z (%) 621.1 (100) [M + Na]⁺. Elemental analysis calcd (%) for C₃₄H₃₈N₄O₂Zn C, 61.55; H, 6.22; N, 8.77. Found C, 61.37, H 5.89, N 8.18.

3.2.3 [Zn-(L3)₂] (3)

The reaction of ligand **L3** (0.30 g, 0.919 mmol) and Zn(OAc)₂·2H₂O (0.106 g, 0.483 mmol) in ethanol furnished complex **3** as a white powder. Yield 72%. Melting point: 228 – 230 °C. ¹H NMR (CDCl₃, 400 MHz): δ (ppm) 1.19 (d, ³J_{H,H} = 6.88 Hz, 12H, ⁱPr-CH₃), 1.24 (d, ³J_{H,H} = 6.68 Hz, 12H, ⁱPr-CH₃), 3.21 (qn, ³J_{H,H} = 6.61, 4H, ⁱPr-CH_{methine}), 3.78 (s, 6H, OCH₃), 6.85 - 6.94 (m, 6H, Ar), 7.10 (dd, ³J_{H,H} = 2.87 Hz 2H, Ar), 7.20 (d, ³J_{H,H} = 7.72 Hz, 4H, Ar), 7.35 (d, ³J_{H,H} = 7.74 Hz, 2H, Ar), 8.23 (s, 2H, NCHN). ¹³C NMR (CDCl₃, 400 MHz): δ (ppm) 24, 25, 28.3, 54.9, 110.9, 116.9, 121.2, 121.6, 123.7, 129.7, 135.9, 138.5, 145.2, 150.3. IR: ν (cm⁻¹) 2963 (m), 1739 (m), 1582 (s), 1499 (m), 1462 (m), 1401 (w), 1312 (w), 1227 (m), ESI-TOF MS: m/z (%)

737.4 (100) $[M + Na]^+$. Elemental analysis calcd (%) for $C_{40}H_{50}N_4O_4Zn$: C, 67.07; H, 7.04; N, 7.82. Found: C, 67.12; H, 6.88; N, 7.94.

3.2.4 $[Zn-(L4)_2]$ (**4**)

The reaction of ligand **L4** (0.30 g, 0.919 mmol) and $Cu(OAc)_2 \cdot 2H_2O$ (0.078 g, 0.394 mmol) in ethanol furnished complex **4** as a white powder. Yield 60%. Melting point 240 – 243 °C. 1H NMR ($CDCl_3$, 400 MHz): δ (ppm) 2.32 (s, 6H, CH_3), 2.37 (s, 6H, CH_3), 3.78 (s, 6H, OCH_3), 7.04 - 7.22 (m, 10H, Ar), 7.71 - 7.74 (d, $^3J_{H,H} = 9.8$ Hz, 4H, Ar), 7.98 (s, 2H, NCHN). ^{13}C NMR ($CDCl_3$, 400 MHz): δ (ppm) 17.7, 18.4, 23.9, 127.6, 128.5, 129.0, 144.7, 148.2. IR: ν (cm^{-1}) 2949 (w), 1614 (s), 1579 (s), 1468 (m), 1228 (m), ESI-TOF MS: m/z (%) 626.34 (100) $[M + Na]^+$. Elemental analysis calcd (%) for $C_{32}H_{34}N_4O_4Zn$, C, 63.63; H, 5.67; N, 9.28. Found C, 63.89, H 5.86, N, 9.66

3.2.5 $[Cu-(L1)_2]$ (**5**)

The reaction of ligand **L1** (0.30 g, 0.919 mmol) and $Cu(OAc)_2 \cdot 2H_2O$ (0.078 g, 0.394 mmol) in ethanol furnished complex **5** as a brown powder. Yield 76%. Melting point: decompose above 238 °C. IR ν 3064 (w), 2960 (s), 2867 (w), 1664 (m), 1620 (s), 1461(m), 1326 (w), 1290 (w), 1254 (w). ESI-TOF MS: m/z (%) 844.6 (100) $[M + Na]^+$. Elemental analysis calcd (%) for $C_{50}H_{70}CuN_4O_2$: C, 73.00; H, 8.58; N, 6.81. Found: C, 73.52; H, 8.39, N, 6.44.

3.2.6 $[Cu-(L2)_2]$ (**6**)

The reaction of ligand **L2** (0.30 g, 0.788 mmol) and $Cu(OAc)_2 \cdot 2H_2O$ (0.076 g, 0.394 mmol) in ethanol furnished complex **6** as a brown powder. Yield 76%. Melting point: decompose above 205 °C. IR ν 3018 (w), 2918 (w), 1608 (s), 1583 (s), 1466 (m), 1390 (w), 1296 (w), 1205 (m), ESI-TOF MS: m/z (%) 621.32(100) $[M + Na]^+$. Elemental analysis calcd (%) for $C_{34}H_{38}N_4O_2Cu$, C, 63.05; H, 6.50; N, 8.40. Found C, 62.79, H 6.83, N 8.82

3.2.7 $[Cu-(L3)_2]$ (**7**)

The reaction of ligand **L3** (0.30 g, 0.919 mmol) and $Cu(OAc)_2 \cdot 2H_2O$ (0.096 g, 0.483 mmol) in ethanol furnished complex **7** as a brown powder. Yield 79%. Melting point: decompose at 235 °C. IR ν 2962 (m), 2868 (w), 1620 (s), 1589 (m), 1494 (w), 1456 (m), 1405 (w), 1312 (w), 1224 (m). ESI-TOF MS: m/z (%) 736.4 (100), $[M + Na]^+$. Elemental analysis calcd (%) for $C_{40}H_{50}N_4O_4Cu$, C, 67.25; H, 7.05; N, 7.84. Found: C, 67.15; H, 6.75; N, 7.83.

3.2.8 [Cu-(L4)₂] (8)

The reaction of ligand **L4** (0.30 g, 0.919 mmol) and Cu(OAc)₂·2H₂O (0.078 g, 0.394 mmol) in ethanol furnished complex **8** as a brown powder. Yield 66%. Melting point: decompose at 205 °C. IR ν 2949 (w), 1612 (s), 1584 (s), 1469 (m), 1228 (m), ESI-TOF MS: m/z (%) 624.1 (100), [M + Na]⁺. Elemental analysis calcd (%) for C₃₂H₃₄N₄O₄Cu, C, 61.97; H, 5.85; N, 9.03. Found C, 61.73, H 5.90, N, 8.84.

3.3 Polymerization of ϵ -caprolactone and L-lactide

All manipulations were performed under an argon inert atmosphere using Schlenk techniques. The initiator and benzyl alcohol co-initiator in a mole ratio of 1:1 were dissolved in toluene (2 ml) and the mixture stirred at 110 °C for 10 mins. Thereafter, the required amount of monomer (ϵ -CL or L-LA) in toluene (1 ml) was then added. Samples for kinetic experiments were withdrawn at regular intervals and quenched quickly by dissolving in cooled CDCl₃ in an NMR tube. The quenched samples were then analyzed by ¹H NMR spectroscopy to determine the extent of polymerization. The percentage conversion was obtained by considering the ϵ -CL monomer protons signal intensities at 4.2 ppm (I_{4.2}) and OCH₂ protons signal intensities at 4.0 ppm (I_{4.0}) from PCL and evaluated using equation (1).

$$[\text{Polymer}]_t/[\text{monomer}]_0 \times 100 = I_{4.0}/(I_{4.2} + I_{4.0}) \times 100 \quad (1)$$

For PLA, the integration values of the methine proton of the monomer and that of the polymer were used to calculate the percentage conversion using the equation (2).

$$[\text{Polymer}]_t/[\text{monomer}]_0 \times 100 = I_{\text{CHmonomer}}/(I_{\text{CHmonomer}} + I_{\text{CHpolymer}}) \times 100 \quad (2)$$

The observed rate constants were extracted from the slope of the line of best fit from the plot of $\ln([M]_0/[M]_t)$ vs time.

3.4 Polymer characterization by size exclusion chromatography (SEC)

Molecular weights and polydispersity indexes were determined by size exclusion chromatography (SEC) at Stellenbosch University. The samples were dissolved in tetrahydrofuran (THF) stabilized with butylated hydroxytoluene (BHT) giving a sample with a concentration of 2 mg ml⁻¹. Sample solutions were filtered *via* a syringe through 0.45 mm nylon filters before being subjected to analysis. The SEC instrument consists of a Waters 1515 isocratic. HPLC pump, a Waters 717plus auto-sampler, a Waters 600E Paper system controller (run by Breeze Version 3.30 SPA) and a Waters in-line Degasser AF. A Waters 2414 differential refractometer was used at 30 °C in series along with a Waters 2487 dual wavelength absorbance UV/Vis detector operating at variable wavelengths. THF (HPLC grade stabilized with 0.125% BHT) was used as the eluent at flow rates of 1 ml min⁻¹. The column oven was kept at 30 °C and the injection volume was 100 µl. Two PLgel (Polymer Laboratories) 5 mm Mixed-C (300 x 7.5 mm) columns and a pre-column (PLgel 5 mm Guard, 50 x 7.5 mm) were used. Calibration was done using narrow poly-styrene standards ranging from 580 to 2 x 10⁶ g/mol. All molecular weights were reported as polystyrene equivalents.

3.5 Single-crystal X-ray diffraction

Crystal evaluation and data collection was done on a Bruker Smart APEXII diffractometer with Mo K α radiation ($\lambda = 0.71073 \text{ \AA}$) equipped with an Oxford Cryostream low temperature apparatus operating at 100 K for all samples. Reflections were collected at different starting angles and the APEXII program suite was used to index the reflections [17]. Data reduction was performed using the SAINT [18] software and the scaling and absorption corrections were applied using the SADABS [19] multi-scan technique. The structures were solved by the direct method using the SHELXS program and refined using SHELXL program [20]. Graphics of the crystal structures were drawn using OLEX² software [21]. Non-hydrogen atoms were first refined isotropically and then by anisotropic refinement with the full-matrix least squares method based on F^2 using SHELXL [20]. The crystallographic data and structure refinement parameters for complexes **3** and **7** are given in Table 1.

Table 1. The summary of X-ray crystal data collection and structure refinement parameters for complex **7**

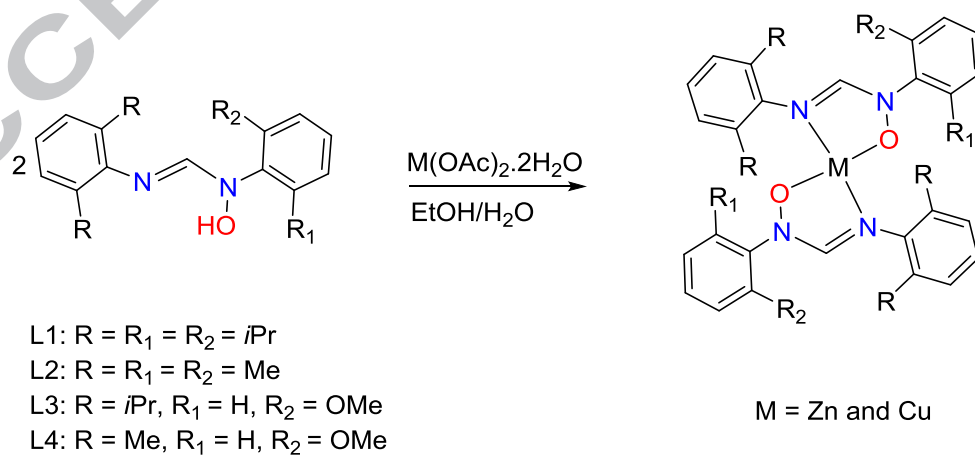
	3	7 .CH ₂ Cl ₂
Empirical formula	C ₄₀ H ₅₀ N ₄ O ₄ Zn	C ₄₀ H ₅₂ Cl ₂ CuN ₄ O ₄
Formula weight	716.21	884.23
T(K)	173(2)	173(2) K
$\lambda(\text{\AA})$	0.71073	0.71073 \AA

Crystal system	Orthorhombic	Monoclinic
Space group	<i>Fdd</i> ₂	<i>P2</i> ₁ / <i>n</i>
<i>a</i> (Å)	33.4780(9)	10.1354(2)
<i>b</i> (Å)	46.5230(18)	11.1941(3)
<i>c</i> (Å)	9.8072(3)	19.1032(9)
<i>a</i> , <i>β</i> , <i>γ</i> (°)	90, 90, 90	90, 90.1610(10), 90
<i>V</i> (Å ³)	15274.7(9)	1645.06(19)
<i>Z</i>	16	2
ρ_{calc} (mg/m ³)	1.246	1.355
μ (mm ⁻¹)	0.687	0.795
<i>F</i> (000)	6080	926
Crystal size (mm)	0.190 × 0.170 × 0.130	0.290 × 0.250 × 0.220
θ range for data collection (°)	1.751 - 27.533	2.109 to 25.366
Index ranges	-43 ≤ <i>h</i> ≤ 43 60 ≤ <i>k</i> ≤ 60 -12 ≤ <i>l</i> ≤ 12	-12 ≤ <i>h</i> ≤ 12 -13 ≤ <i>k</i> ≤ 13 -21 ≤ <i>l</i> ≤ 21
Reflections collected	124701	40512
Independent reflections	8789 [<i>R</i> _{int} = 0.0234]	3860 [<i>R</i> _{int} = 0.0173]
Completeness to $\theta = 25.24^\circ$ (%)	99.9	97.2
Data/restraints/parameters	8789/1/442	3860 / 0 / 255
Goodness-of-fit (GOF) on <i>F</i> ²	1.038	1.054
Final <i>R</i> indices [<i>I</i> > 2σ(<i>I</i>)]	<i>R</i> ₁ = 0.0202, <i>wR</i> ₂ = 0.0531	<i>R</i> ₁ = 0.0386, <i>wR</i> ₂ = 0.0919
<i>R</i> indices (all data)	<i>R</i> ₁ = 0.0218, <i>wR</i> ₂ = 0.0541	<i>R</i> ₁ = 0.0401, <i>wR</i> ₂ = 0.0930
Largest diff. peak and hole (e Å ⁻³)	0.234 and -0.278	1.308 and -1.048

4.0 Results and discussion

4.1 Synthesis of *N*-hydroxy-*N,N'*-diarylformamidine ligands and their Zn(II) and Cu(II) complexes

The *N*-hydroxy-*N,N'*-diarylformamidine ligands **L1** - **L4** were synthesized from a previously reported method in which the *N,N'*-diarylformamidine precursors[22] were *N*-oxidized with *m*-MCPBA [23]. Their identity was confirmed using NMR, mass spectrometry and elemental analysis. Reaction of **L1** - **L4** with hydrated Zn(II) and Cu(II) acetates gave metal complexes supported by two ligands where the acetate anions are displaced from the coordination sphere. The following complexes, [Zn-(**L1**)₂] (**1**), Zn-(**L2**)₂] (**2**), Zn-(**L3**)₂] (**3**), [Zn-(**L4**)₂] (**4**), [Cu-(**L1**)₂] (**5**), [Cu-(**L2**)₂] (**6**), [Cu-(**L3**)₂] (**7**), [Cu-(**L4**)₂] (**8**) were obtained as air stable solids in good yield (64 – 84%) (see Scheme 1). The Zn(II) complexes were obtained as white solids while Cu(II) complexes were obtained as brown solids. The melting points for Zn(II) complexes ranges from 189 – 245 °C compared to 130 – 154 °C for the ligands. Cu(II) complexes did not exhibit a defined melting points but rather, they decomposed between (205 – 245 °C). The general molecular formula of the complexes M(L)₂ (L = ligands **L1** - **L4**) was validated by microanalytical data which clearly showed that the metal:ligand ratio is 1:2. The stoichiometry was further corroborated by mass spectrometry data. For example, complex **1** showed a base peak at *m/z* 847.59 which correspond to [Cu(**L1**)₂+Na]⁺ (Fig. S1a). Similar results were also obtained for complexes **2** - **8** and the ESI mass spectra are shown in Fig. S1b - h. It is noteworthy that monomeric forms of **1** and **2** with symmetrically 2,6-substituted *N*-hydroxy-*N,N'*-diarylformamidine ligands appear in literature and will not be discussed in detail [24].



Scheme 1. Synthesis of Zn(II) and Cu(II) *N*-hydroxy-*N,N'*-diarylformamidine complexes

4.2 IR and NMR spectroscopy

The IR spectra of complexes **1** – **8** display a general shift of the azomethine (C(H)=N) symmetric stretch toward lower frequencies as compared to free ligands indicative of imine nitrogen participation in coordination (see Table 2). For example, the C=N symmetric stretching frequency in complex **1** appeared at 1607 cm⁻¹ as compared to 1610 cm⁻¹ in ligand **L1**. The observed shifts are due to reduced π -electron density upon coordination rendering the C=N bond to have a partial single bond character hence resonating at lower frequencies. The summarized data of shifts for other complexes are shown in Table 2.

The ¹H NMR and ¹³C NMR of complexes **1** - **4** were recorded in CDCl₃ and are provided in the supplementary section as Fig. S2a - h. Typical aliphatic signals resonate in the region 1.0 - 2.29 ppm and could be seen for all Zn(II) complexes. In complex **1** the ⁱPr methyl signals appear as four doublets compared to the free ligand due to their stereochemical nature and interaction with the metal center. The azomethine proton NC(H)=N signals are shifted up field in complex **1** – **4** compared to the free ligands **L1** – **L4** (see Table 1) because they are shielded by the coordinating metal. The shielding is more pronounced with a significant proton resonance shift for unsymmetrical substituted complexes **3** and **4** as compared to complex **1** and **2**. Also, ¹³C NMR spectra (Fig. S2e - h) showed that azomethine carbon signal is shifted downfield due to metal coordination and appears around 150 ppm which contrasts with 147-148 ppm for free-ligands.

Table 2. IR (azomethine C=N symmetry stretch frequency) and NMR (azomethine proton resonance peaks) for ligands and complexes, respectively

Complex	IR $\nu(\text{C}=\text{N})$ cm ⁻¹			NMR σ (ppm) NC(H)N		
	Ligand	Complex	$\Delta\nu$	Ligand	Complex	$\Delta\sigma$
1	1610	1607	3	7.22	7.20	0.01
2	1612	1598	14	7.34	7.31	0.03
3	1655	1582	73	8.90	8.33	0.57
4	1648	1579	69	8.42	8.25	0.20

5	1620	1610	10	-	-
6	1612	1608	4	-	-
7	1655	1620	35	-	-
8	1648	1612	36	-	-

4.3 Molecular structures of complexes **3** and **7**

The molecular structures of complexes **3** and **7** were determined by single crystal X-ray diffraction. The crystals were obtained by slow diffusion of diethyl ether to saturated dichloromethane complex solutions. The molecular structures are shown in Fig. 2 and 3 while selected interatomic distances, bond and torsional angles are listed in Table 3.

The asymmetric unit of complex **3** contains one complex molecule while for complex **7**, consist of one complex molecule and dichloromethane co-solvent. In both cases, the complex molecule consists of a metal ion coordinated to two ligands. The acetate anions from the metal salts are displaced from the coordination sphere. The ligands coordinate *via* the imine *N* and hydroxy *O* in a bidentate fashion resulting in pentacyclic metallacycles which are comparable to other *N,O* bidentate ligands [25]. This confers a distorted tetrahedral and a square planar geometry around the Zn(II) and Cu(II) metal centers, respectively. The bond angles around the metal center in complex **3** range from 108.77(6) – 146.62(6)° while in complex **7** are 83.93(7) and 96.07(7)° (Table 3) and which is a deviation from those of regular tetrahedron or square planar geometries, respectively. Similar values have been reported in literature for related structures.[24a,26].

In complex **3**, the metallacycle plane is nearly perpendicular to the 2,6-disubstituted aromatic ring planes with dihedral angles between 79.9(3) – 92.5(3)° while nonplanar to the methoxy substituted rings with dihedral angles between 17.2(4) – 142.2(3)°. In complex **7**, the 2,6-disubstituted and methoxy substituted phenyl ring planes have dihedral angles of 82.7(2)° and 53.1(3)° with respect to the pentacyclic chelate rings. In both cases, the difference in dihedral angles between 2,6-ⁱPr- and MeO- substituted rings is due to steric repulsions induced by bulkier ⁱPr groups.

The mean Zn—O and Zn—N bond lengths in complex **3** are 1.998(2) and 1.984(2) Å, respectively which are consistent with reported structures coordinating through the imine nitrogen [24a]. On the other hand, they are smaller compared to reported related Schiff base complexes [27]. For instance Wu *et al* [28] reported an average Zn—N_{imine} bond length of 2.106(3) Å with Salen-type ligands. The Zn(1)—O(3)_{methoxy} distance in complex **3** (2.477(2) Å) is slightly longer compared to other structures that have been reported in literature [29].

In complex **7**, the Cu(1)—O(1)—N(1)—C(13) torsion angle confirms the out-of-plane displacement of 1.0(2)° from the chelate ring with respect to the N—O—Metal orbitals. The average bond distances of Cu—O (1.9264(14) Å) and Cu—N_{imine} (1.9399(17) Å) are consistent with other reported structures reported by Okazawa *et al* [30] for pyridyl nitroxide supported Cu(II) complexes with Cu—O bond distance between (1.9316(19) – 1.9491(18) Å) and Cu—N_{pyr} (1.9281) Å. The C—N bond distances are almost identical in both structures, indicative of delocalized π -electron density over the —N=C—N— backbone.

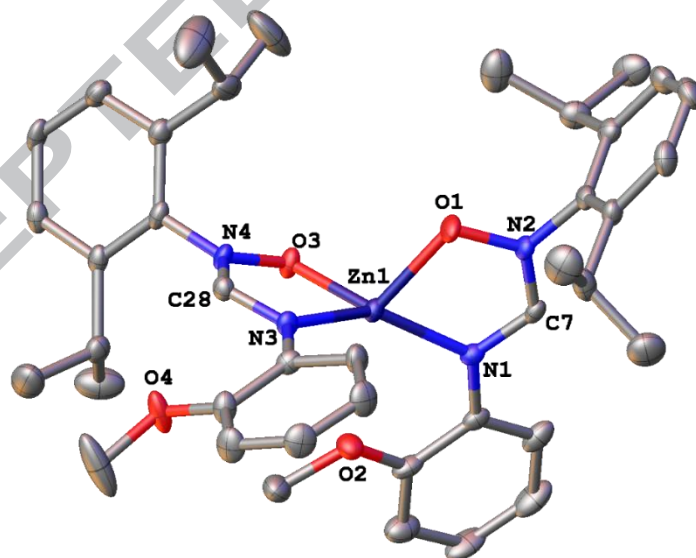


Fig. 2. X-ray crystal structure of complex **3** with thermal ellipsoids drawn at 50% probability level and hydrogen atoms have been omitted for clarity

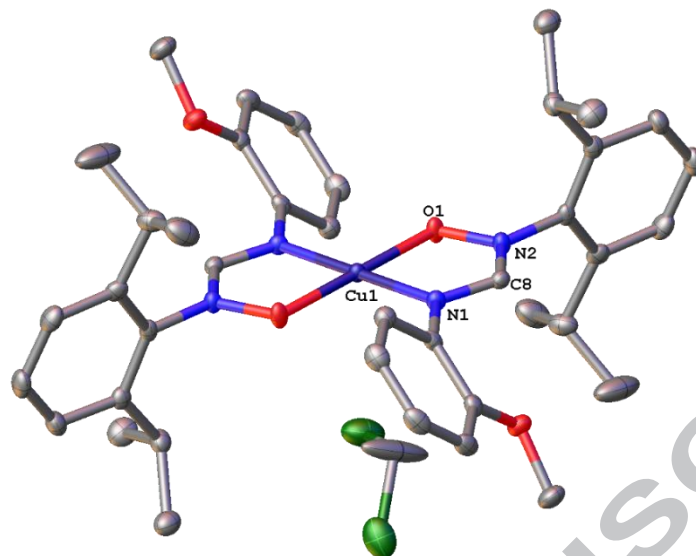


Fig. 3. X-ray crystal structure of complex **7** with thermal ellipsoids drawn at 50% probability level and hydrogen atoms have been omitted for clarity

Table 3. Selected bond lengths and angles for complexes **3** and **7**

	3	7
<i>Bond lengths [Å]</i>		
M—N	1.980(3) – 1.988(2)	1.9399(17)
M—O	1.982(2) – 2.014(2)	1.9264(14)
C—N	1.314(4) – 1.319(4)	1.315(3) – 1.316(3)
<i>Angles [°]</i>		
O—M—N(cone)	81.48(5) – 83.84(5)	83.93(7) – 96.07(7)
O—M—O	112.27(6)	180(1)
N—M—N	146.62(6)	180(2)
O—M—N	108.77(6) – 122.79(6)	
<i>Dihedral angles [°]</i>		
C—N—O—M	1.3(2) – 7.0(2)	1.0(2)
N—C—N—M	1.3(2) – 4.9(2)	1.4(2)
2,6 ⁱ PrPh—(NO)	79.70(2) – 92.60(2)	82.7(2),
2-MeOPh—(NM)	17.2(2) – 141.85(16)	53.1(3)

4.4 Ring opening polymerization of ϵ -caprolactone and L-lactide

Complexes **1 - 8** were investigated for their catalytic activity in polymerization of ϵ -caprolactone and L-lactide. Preliminary studies were done in bulk at 110 °C using 100:1 monomer to catalyst ratio. Longer induction periods, greater than 24 h, were observed for complexes **1 - 8** with the most active being complex **2**, achieving only less than 5% monomer conversion. This can be attributed to three main reasons, namely catalyst conformational changes to form a monomer-catalyst transition state [28], heat transfer and catalyst dissociation to less reactive species [29]. There were no further efforts to try and probe the nature of the induction periods in our system.

To speed up the initiation process an external nucleophile was then added as a co-initiator. The polymerization of ϵ -CL was then carried out in toluene at 110 °C using benzyl alcohol as a co-initiator with a [M/I/BnOH] mole ratio of 100:1:1. Complexes **1 - 8** showed increased catalytic activity with complex **2** still exhibiting superior activity. There was virtually no induction period for Zn(II) complexes **1 - 4** (Fig S3a) in the presence of co-initiator, signifying the existence of reactive catalytic species from the start. However, for Cu(II) complexes **5 - 8** the induction period was reduced with complex **6** being the most active among the Cu(II) series having an induction period of about 10 h (Fig. 3b). The complexes behave as catalysts with the induction periods involving both the monomer and the co-initiator activation, hence they can be interchangeably referred to as catalysts or initiators. Monomer conversions between 90 – 99% were observed within 22 – 125 h for complexes **1 - 8** (Fig. S3a). Complex **2** which was the most active was used to probe the polymerization of L-LA with monomer equivalent between 100 – 300. Conversion of up 99% were achieved within 14 – 19 h for different L-LA monomer concentrations. The summary of results is presented in Table 4 and 5.

The Zn(II) catalyst, **1 - 4**, were more active than the Cu(II) analogues, **5 - 8**, in solution polymerization of ϵ -CL. For example, in a relative comparison complexes **3** and **7** (entries 5 and 11 in Table 4) a conversion of about 99% was achieved within 68 h for complex **3** while complex **7**, 115 h of reaction time was needed. A more active Cu(II) diketimate system developed by Whiteborne *et al* [30] is an exception where full conversion of lactides was obtained within 1 h at room temperature. There are two possible explanations for the difference in activity. Firstly, greater electrophilicity of Zn(II) as compared to Cu(II) plays an important

part in monomer binding to the former more readily, hence more active. Secondly, the stronger Cu—O bond compared to Zn—O (see table 2), does not readily break to initiate the polymerization process. . Although the M—O bond distances are comparable to those with auxiliary alkoxides and acetate, which are normally active initiators. [14a,30-31], inclusion of the oxygen in the ligand skeleton seem to make the bond less labile due to the chelating effect.

Table 4. Summary of polymerization data of ϵ -CL by complexes **1 – 8**

Entry	Complex	[M/cat]	^c Time (h)	^c Conv (%)	^b Mw(calc)	^d Mw _(GPC)	^e PDI	<i>k</i> _{app}
1	1	100:1	32	99	11286	1884	1.23	0.1519
2	1	300:1	36	97	33174	2667	1.45	
3	2	100:1	24	98	11172	2239	1.30	0.1751
4	2	300:1	28	99	33858	2909	1.40	
5	3	100:1	68	99	11286	2088	1.42	0.0693
6	3	300:1	80	99	33858	2184	1.24	
7	4	100:1	73	96	10944	1512	1.22	0.0386
8	4	300:1	96	95	10830	1939	1.25	
9	5	100:1	94	90	10260	1506	1.38	
10	6	100:1	105	93	10602	2090	1.66	
11	7	100:1	115	97	11058	1039	1.20	
12	8	100:1	125	96	10944	1047	1.10	

^aPolymerization conditions: 110 °C, 3.0 ml of toluene as the solvent, [M]₀:[catalyst]₀:[BnOH]₀ = 100:1:1. ^cDetermined from NMR. ^bCalculated theoretical Mw. ^{d,e}Determined by GPC relative to polystyrene standards in THF. ^dExperimental Mw was calculated considering Mark–Houwink’s corrections of 0.56.

Table 5. Effect of catalyst concentration on polymerization of L-lactide by complex **2**

Entry	[M/Cat]	Time (h)	^f Conv (%)	^g Mw(calc)	^h Mw _(GPC)	ⁱ PDI
-------	---------	----------	-----------------------	-----------------------	----------------------------------	------------------

1	100:1	14	99	11286	1190	1.5
2	200:1	16	99	22572	1742	1.71
3	300:1	19	97	33174	2274	1.71

Polymerization conditions: 110 °C, 3.0 ml of toluene as the solvent, [Cat]₀: [BnOH]₀ = 1:1. Percentage conversion from NMR. ^gCalculated theoretical M_w. ^{h,i}Determined by GPC relative to polystyrene standards in THF. Experimental M_w was calculated considering Mark–Houwink’s corrections of 0.58.

4.5 Kinetics of ROP reactions of ε-CL and L-LA

Kinetic studies to ascertain the dependence of reaction rates on monomer concentration were carried out at 110 °C with a [monomer]₀/[catalyst]₀ ratio of 100:1. Non-linear plots of ln([CL]₀/[CL]_t) vs time were obtained for Cu(II) complexes as depicted for complex **5** (Fig. S4) suggesting a second order dependence on monomer concentration. Zn(II) complexes **1** – **4**, exhibited a linear relationship for ln ([M]₀/[M]_t) vs time and the apparent rate constants (*k_{app}*) of polymerization were obtained from the slopes (Fig. 4).. The linearity points to a *pseudo* first-order polymerization reaction with respect to ε-CL or L-LA monomer concentrations. Hence, for *pseudo* first

$$-\frac{d[M]}{dt} = k[M] \quad (3)$$

For a specific monomer concentration ([M]), and constant initial catalyst concentration ([Catalyst]₀), $k = kp[Cat]^x$ where *kp* = rate of chain propagation, Cat = catalyst, and x is the order of reaction. The overall propagation rate (Rp) is expressed as shown in equation (4).

$$Rp = \frac{d[M]}{dt} = kp[M]_0^a [Cat]_0^x \quad (4)$$

In the presence of a co-initiator, in case of benzyl alcohol (BnOH) with initial concentration [BnOH]₀, Rp is expressed as equation (5)

$$Rp = \frac{d[M]}{dt} = kp[M]_0^a [BnOH]_0^b [Cat]_0^x \quad (5)$$

where a and b are orders of reaction with respect to monomer and co-initiator, respectively.

The rate of polymerization of ϵ -CL is comparable to that of L-LA. For instance, in the case of ϵ -CL complex **2** gave an apparent rate constant of 0.2036 h^{-1} (Fig. S5) compared to 0.1751 h^{-1} (Fig. 4). Generally, the 6-membered L-LA heterocyclic ring is more strained as compared to the 7-membered ϵ -CL ring resulting in higher rates of polymerization. The observed low apparent rate constants were also depended on the steric and electronic effects of the catalyst. There was no drastic change in activity between complex **1** (0.1519 h^{-1}), bearing bulky isopropyl substituents and complex **2** ($k_{app} = 0.1751 \text{ h}^{-1}$), with symmetric 2,6-methyl substituents. However, replacing 2,6-substituents with a single *ortho*-methoxyl group on the other phenyl ring resulted in a significant decrease in the activity (**3**, $k_{app} = 0.0693 \text{ h}^{-1}$ and **4**, $k_{app} = 0.0386 \text{ h}^{-1}$). Metal to oxygen interactions of about $2.447(2) \text{ \AA}$ were detected in the molecular structure of complex **3** and can possibly be maintained in solution hence competing with monomer coordination resulting in lower polymerization rates. Generally the apparent rate constants obtained for the complexes **1** – **4** are slightly inferior to other reported systems bearing *N,N,O*-ligating ligands [6a,32] but are comparable to Zn(II) and Cu(II) complexes supported by bis(3,5-dimethyl)pyrazole ligands with rates between 0.090 to 0.286 h^{-1} as reported by Appavoo *et al* [10a].

Reaction variables also influence the polymerization kinetics, hence the effect of varying the monomer concentration on the apparent rate constant was investigated for complex **2**. A constant $[\text{Cat}]_0/[\text{BnOH}]_0$ mole ratio of 1:2 was used while the monomer ratio was varied from 150 to 300. Increasing the monomer to catalyst ratio resulted in decreased rates without an induction period (and Fig. S6). The linearity of the plot of $\ln([\text{CL}]_0/[\text{CL}]_t)$ vs time for complexes **1** - **4** showed a *pseudo* first order dependence on the initial monomer concentration.

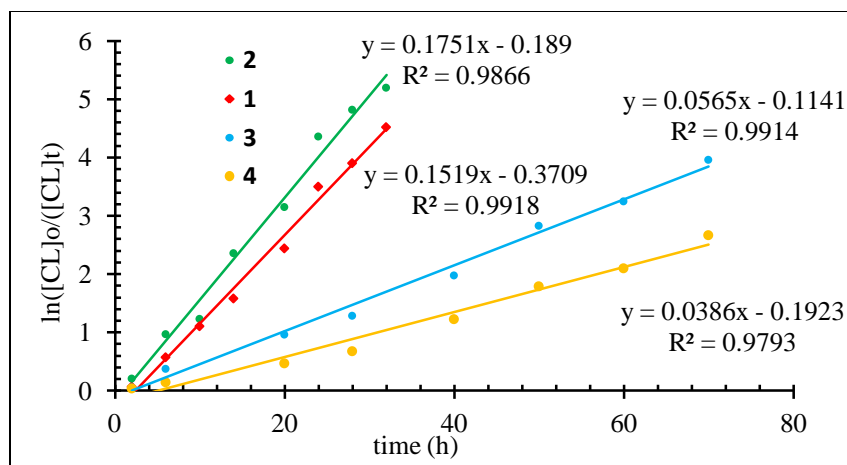


Fig. 4. Plots of $\ln([CL]_0/[CL]_t)$ versus time catalyzed by complexes **1** and **4**. Reaction conditions: $[M]_0:[cat]:[BnOH]_0 = 100:1:1$ solvent: toluene; $T = 110\text{ }^\circ\text{C}$

4.6 Reaction order for ROP of ϵ -CL with respect to co-initiator $[BnOH]_0$ and complex **2**

To establish the order of reaction with respect to the initial co-initiator (BnOH) concentration, the most active complex **2** was chosen and a constant monomer to catalyst ratio of 100:2 was used while varying the co-initiator concentration. The plot of $\ln(k_{app})$ vs $\ln[BnOH]_0$ (Fig. 5) permits the determination of reaction order with respect to benzyl alcohol concentration from the gradient. The extrapolated slope gave a fractional order of 0.49 which shows that multiple steps are involved. To obtain the order with respect to the complex **2**, constant monomer to co-initiator ratio ($[CL]:[BnOH]_0$) of 100:2 was used and the catalyst was varied from 3 mM to 6 mM. The best fit logarithmic linear plot of $\ln(k_{app})$ vs $\ln[2]_0$ (Fig. 5) gave a slope of 1.1 indicating first order reliance on catalyst concentration and is comparable to the bis(pyrazolylmethyl)pyridine Zn(II) complex reported by Zikode *et al* [33]. In contrast, fractional reaction orders for the catalyst have also been observed in bulk polymerization due to catalyst aggregation, and dissociation to form reactive species [34]. In addition, a formamidine Zn(II) system showed 0.3 and 0.6 fractional reaction orders [35]. The overall rate equation can be written as shown in equation (5).

$$R_p = \frac{d[CL]}{dt} = k_p[CL]_0^1[BnOH]_0^{0.5}[2]_0^{1.1} \quad (5)$$

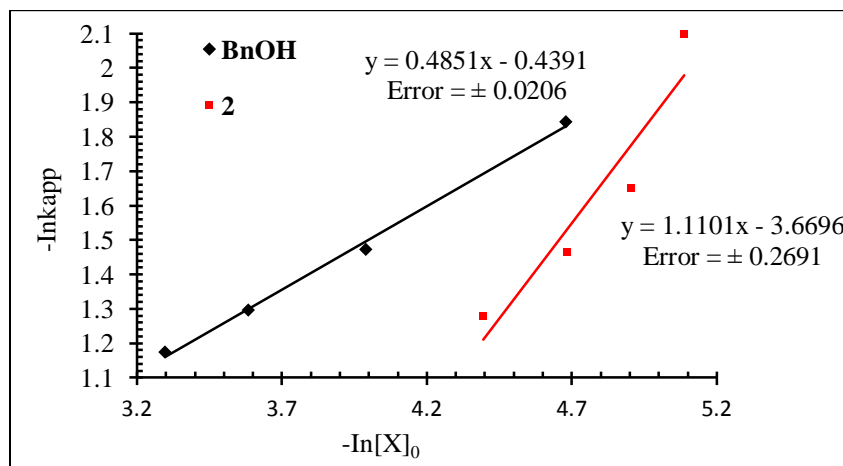


Fig. 5. Plot of $\ln k_{app}$ vs initial concentration of BnOH (black) and complex **2** (red) for determining the order of reaction with respect to co-initiator and catalyst

4.7 Molecular weight and molecular weight distribution of polymers

The molecular weight (M_w) and the molecular weight distributions ($PDI = M_w/M_n$) were determined by gel permeation chromatography (GPC) and compared to the theoretical values. Appropriate Mark–Houwink corrections 0.56 for PCLs and 0.58 PLAs were used. Low molecular weights less than those obtained by NMR were obtained. The observed molecular weight ranged from 1855 - 3999 Da and 1190 - 2274 Da for PCLs and PLAs, respectively (Table 4 and 5). Increasing the monomer to catalyst ratio (having less initiating species) did not yield a significant increase in the molecular weight (Table 4, entries 2, 4, 6 and 8). For instance, complex **4** showed molecular weight increased from 1512 to 1939 Da when the monomer to catalyst ratio was changed (Table 4, entries 7 and 8), a 4% increase with respect to calculated molecular weight. Low molecular weights inferred that the catalysts are less efficient resulting in limited number of chains growing to reach the predicted molecular weights [36].

The observed molecular weights for complexes **1** – **8** are inferior to those reported by Wang *et al* [37], under similar conditions, which ranged from 1300 - 28800 Da. with PDIs less than 1.27. Obuah *et al* [38], also reported low molecular weights between 1480 to 7080 Da in bulk polymerization of ϵ -CL using ferrocenyl(pyrazolyl)- Zn(II) and Cu(II) complexes. Two reasons are possible for the observed low molecular weights. Firstly, the co-initiator can act as a chain

transfer agent causing premature chain termination [39]. Secondly, it can be attributed to inter- and intra-molecular trans-esterification side reactions (back-biting) that cause cyclization and shortening of the propagating polymer chains [40]. Our system appears to be influenced by both scenarios since a co-initiator was added and the presence of small peaks in the ESI-MS spectra of PCL and PLA (Fig. 6 and Fig. S8) matching cyclic polymers were observed. Cyclization normally happens at extended reaction times when the monomer is almost completely depleted and at higher molecular weights where the chains can easily fold [41]. It has been reported that bulk ligands can help in selective coordination of the monomer than the polymer chains to the metal center hence reducing transesterification [42].

Although not significant, symmetry coupled with steric bulkiness of the ligand skeleton seem to have a bearing on the resultant polymer molecular weights. Bulky isopropyl groups in complex **1** and **5** (Table 4 entries ,1 and 9) resulted in slightly lower molecular weights as compared to complexes **2** and **6** (Table 4, entries 2 and 6) with methyl substituents. This is because bulky substituents inhibit monomer interaction with the metal center for activation. This trend contrasts what was observed by Shen *et al* [43] in their study of steric effects in free ligand substituted phenolates samarium complex. They noted that *ortho* bulkier groups repel more and prevented close packing of phenyl rings towards the metal center hence creating ample space for monomer coordination which resulted in increased catalytic activity.

Unsymmetrically substituted complexes **3,4,7** and **8** (Table 4, entries 5, 7, 11 and 12) have lower molecular weights as compared to symmetrically substituted complexes. This could be due to the methoxyl oxygen which is weakly coordinating there by strongly competing with monomer coordination to the metal center. Albeit catalytic activity shown by these complexes, the tendency to produce lower molecular weights polymers limits the system to produce polymers which can be applied in areas where toughness is a requirement. However, they are suitable for drug delivery systems like hydrogels [44].

Polymers obtained from complexes **1 – 8** showed relatively narrow polydispersity indices which ranges between 1.2 and 1.45 and 1.5 and 1.7 for PCLs and PLAs, respectively. Relatively narrow polydispersity indices for PCLs as compared to the PLAs can infer that the polymerization is not well controlled in case of PLAs. Although the polydispersity indices are higher than those anticipated for an ideally living polymerization, however, they are generally

accepted for a controlled polymerization model in case of PCLs.

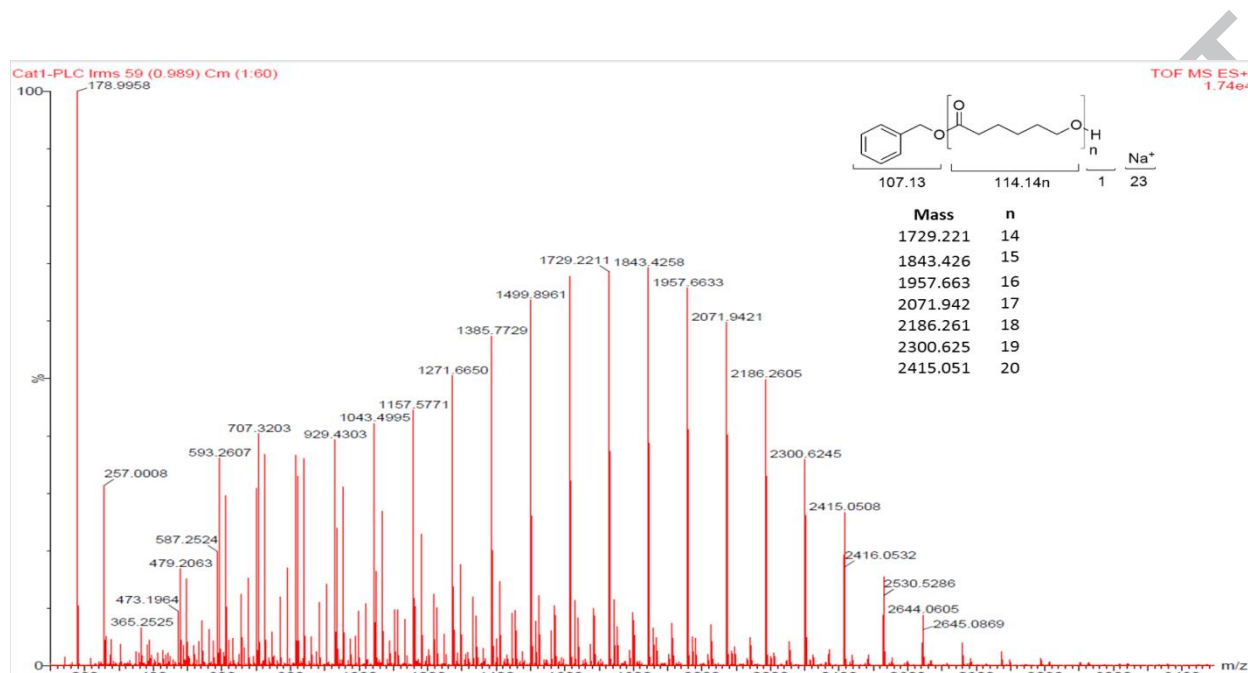


Fig. 6 ESI-MS spectra of PCL obtained from complex **1**, $[\text{CL}]_0:[\text{BnOH}]_0 = 100:1$, $t = 32$ h

4.8 Homo polymer structure, end group and mechanistic analysis

There are two main mechanisms that have been proposed for ROP of cyclic esters using metal alkoxide catalyst, namely; coordination insertion (CIM) and activated monomer mechanisms (AMM) [45]. The AMM utilizes an external added nucleophile while in CIM the nucleophile is integrated as part of the catalyst through a covalent bond to the metal center [45c]. The system under study possess metal-oxygen bonds which are responsible for initiating in ROP therefore, initiation by coordinating ligands cannot be ruled out. NMR and mass spectroscopies were used for an in-depth analysis of the polymer microstructure to establish the initiating group.

Typical ESI-MS spectra for PCL and PLA are shown in Fig. 6 and Fig. S8 and a monotone spreading peaks matching distinctive polymer topology were observed. The mass spectra are characterized by a collection of peaks separated by respective repeating unit molar masses. For PCLs peaks are differentiated by 114.1 Da (single caprolactone fragment, Fig. 6) and for PLA, a peak separation of 72 Da (single lactyl fragment, Fig. S8) was observed. A peak difference of 72

Da points to significant transesterification during the polymerization of L-LA. Analysis ESI-MS of PCL showed a peak at $[M+Na]^+$, (1729.22 Da, Fig. 6) resulting from a polymer with degree of polymerization (DP = 14) having BnO- and -OH terminal groups. From Fig S8 the ion peak at 817.15 Da ($[M+Na]^+$) matches a PLA polymer having DP of 10 with similar terminal groups.

1H NMR spectroscopy was used to further interpret and confirm the mechanism of polymerization. Analysis of the 1H NMR spectra of polymers (Fig. 7 and 12) showed no signals of free *N*-hydroxy-*N,N'*-diarylformamidinium ligand moiety. This is an indication that the ligand moiety is not part of the polymer chain hence it was not involved in the initiation step as was initially proposed. In contrast to amido ligands by Liu and Ma [9e], the chelating amido ligands were capable of initiation ROP and were part of the growing polymer chains. To get further insight about ligand lability in solution a mixture of complex **2** and BnOH was analyzed by 1H NMR in C_6D_6 . Two new singlet signals at 4.3 and 4.6 ppm were observed due to methylene protons of free and coordinated benzyl alcohol (Fig. S9). No signals were observed of the free ligand hence the complex maintain its structure in solution.

The initiating and chain-end groups in the polymers, were deduced from 1H NMR and ESI-MS-spectra (Fig. 7 - 12). Analysis of 1H NMR spectra (Fig. 7 and 10) showed the presence of a triplet signals at 3.66 and 4.88 ppm for PCL and PLA, respectively. The signals are ascribed to the methylene protons neighboring the hydroxyl termini end. Also, the singlet at 5.2 ppm from the benzoyl methylene protons confirmed that the polymers were end capped with a benzyl ester. This support that the propagation mechanism was *via* the insertion of a benzyloxy group into the oxygen-acyl bond of the monomer. Kinetics investigations together with NMR and ESI-MS data for the ROP of ϵ -CL for complex **2** and co-initiator lead us to conclude that an activated monomer mechanism is in operation as shown in Fig. 9. This observation is consistent with other reported literature work [34b,45c,46].

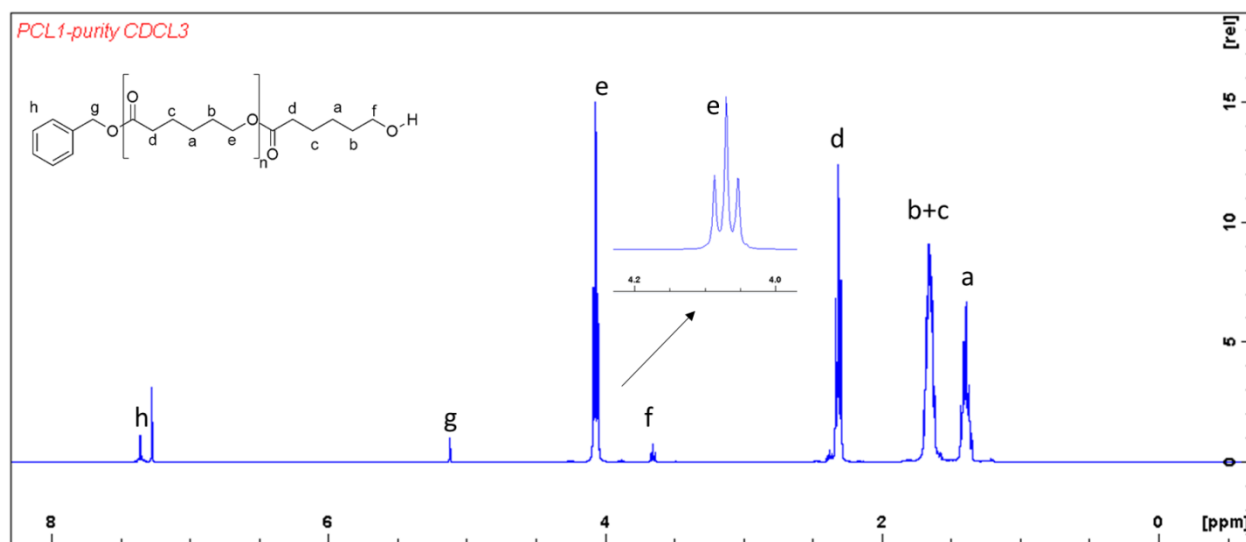


Fig. 7. The ¹H NMR spectrum of PCL initiated by complex **1**/BnOH. Reaction conditions: [CL]₀: [BnOH]₀ = 100:1, solvent: toluene, T = 110 °C

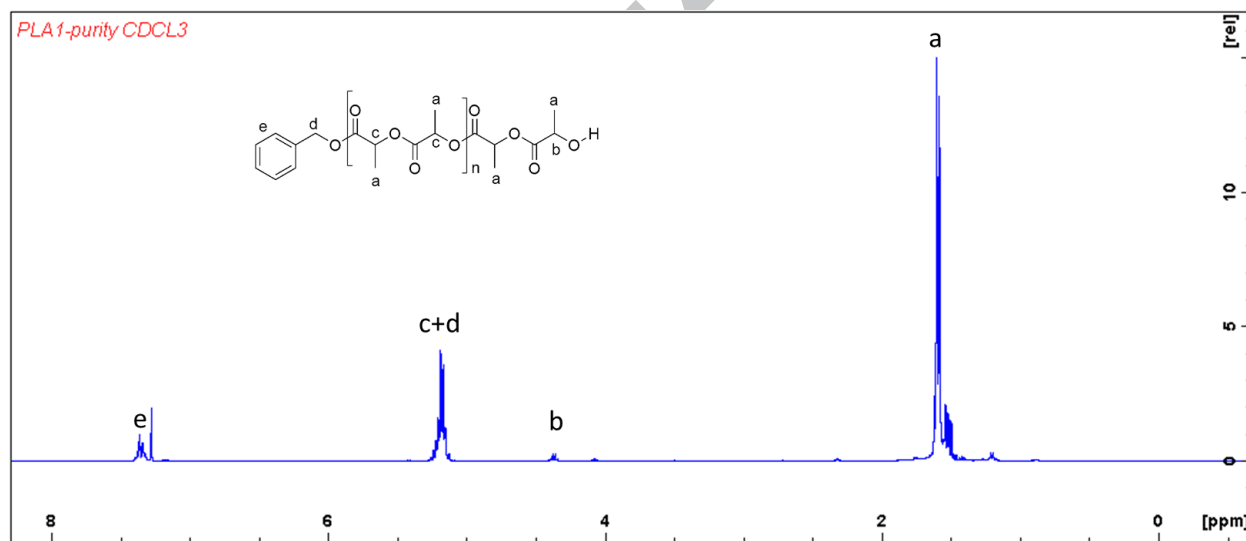


Fig. 8. The ¹H NMR spectrum of PLA initiated by complex **1**/BnOH. Reaction conditions: [LA]₀: [BnOH]₀ = 100:1, solvent: toluene, T = 110 °C

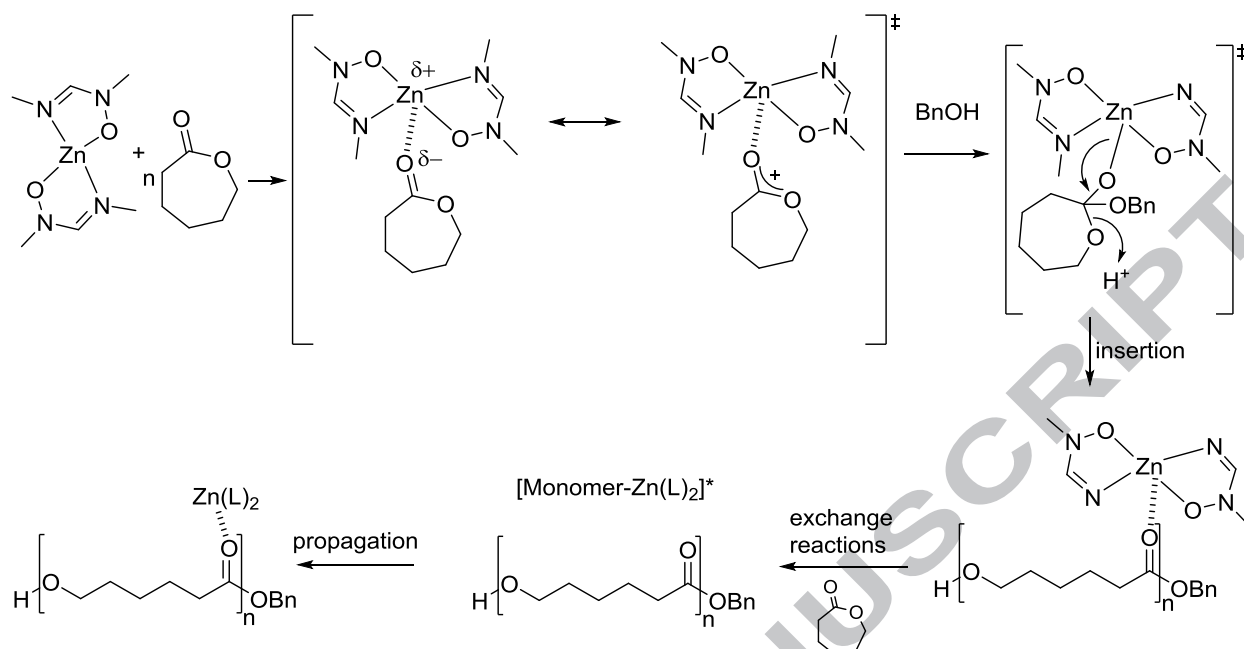


Fig. 9. Proposed monomer activation mechanism for the polymerization of ϵ -caprolactone

4.9 Copolymerization of *L*-lactide and ϵ -caprolactone using complex 2

The physical properties of polyesters derived homo-polymers can limit their applicability, thus require modification. One such strategy is copolymerization which results in block polymers with improved properties. Complex 2 was used in the co-polymerization of ϵ -CL and *L*-LA and PCL-*b*-PLA block copolymers were obtained and characterized by NMR. The absence of a signal due to end group functionality methylene protons (HOCH₂-O-) at 3.65 ppm in ¹H NMR spectra from the homo-polymer (Fig. S10) showed that a block copolymer was formed. The two methylene proton signals at 4.16 and 4.06 ppm (Fig. S10 inset) showed a CL-LA homojunction compared to a CL-CL homojunction (4.06 ppm) (Fig. 7 inset). The PCL methylene protons in proximity to the PLA chain are slightly shifted giving two signals. This is corroborated by ¹³C NMR (Fig.S11) where two carbonyl carbon signals at 169.5 and 173.6 ppm are present suggesting the sequences LLC and LCC originating from the homo-sequence LA-LA-LA and CL-CL-CL, respectively. Generally, it is more probable to form a PCL-*b*-PLA block copolymer than the PLA-*b*-PCL because the preformed PCL prepolymer is an effective initiator than the PLA, therefore, monomer addition sequence must be considered.

5.0 Conclusion

Zn(II) and Cu(II) *N*-hydroxyformammidine complexes were effectively synthesized and were obtained in reasonable yield (64 – 84 %). All the complexes were characterized by IR, NMR, mass spectroscopy and elemental analysis. The molecular structures of complexes **3** and **7** were determined by single crystal X-ray diffraction analyses. In both structures, the coordination sites are occupied by imino *N* and hydroxyl *O* donor atoms from the chelating ligands. The geometry around the metal center in complex **3** is distorted tetrahedral while in complex **7** is square planar. The ROP of ϵ -CL and *L*-LA catalyzed by complexes **1** - **8** on their own showed longer induction periods with complex **2** achieving only 5% conversion within 24 h. Solution polymerization in toluene in the presence of a benzyl alcohol as co-initiator, complexes **1** – **8** proved to be active achieving monomer conversion up to 99% within 22 – 125 h. The more electrophilic Zn(II) complexes were more active as compared to the Cu(II) analogs. The polymerization of ϵ -CL showed controllable characteristics as shown by relatively low PDIs ranging from 1.1 – 1.6 although low molecular weights less than 2909 Da were observed. The complexes exhibited low activity with complexes **1** – **4** achieving apparent rate constants (k_{app}) between 0.0386 – 0.1751 h⁻¹. Plots of $\ln([CL]_0/[CL]_t)$ vs time for complexes **5** – **8** were nonlinear showing the non-living characteristic of these systems. Symmetry coupled with steric effects seem to have an effect on the activities of the complexes. Complexes with symmetric 2,6-substituents were more active than the unsymmetrical ones possessing 2-methoxy on the other phenyl ring. A monomer activation mechanism was proposed as supported by the end-group analysis using ¹H NMR spectroscopy and ESI-TOF mass spectrometry. To improve the activity further studies might include a dual catalytic approach where a Brønsted base is added to activate the catalyst/co-initiator [47] as well as ligand modification.

Acknowledgements

The authors would like to thank College of Agriculture, Science and Engineering, University of KwaZulu-Natal, National Research Foundation (NRF) of South Africa and German Academic Exchange Service (DAAD) for financial support.

Appendix A: Supplementary data

CCDC 1573015 and 1558186 (for **3** and **7** respectively) contains the supplementary crystallographic data for all structures in this paper. These data can be obtained free of charge via <http://www.ccdc.cam.ac.uk/conts/retrieving.html>, or from the Cambridge Crystallographic Data Centre, 12 Union Road, Cambridge CB2 1EZ, UK; fax: (+44) 1223-336-033; or e-mail: deposit@ccdc.cam.ac.uk. Supplementary data associated with this article can be found, in the online version, at

Reference

- [1] V. Mittal, *Renewable Polymers: Synthesis, Processing, and Technology*, John Wiley & Sons, Hoboken, NJ, 2012.
- [2] (a) M. Kashif, B.-m. Yun, K.-S. Lee, Y.-W. Chang, *Mater. Lett.*, 166 (2016) 125; (b) K. Jelonek, J. Kasperczyk, *Polimery*, 58 (2013) 858.
- [3] S. Hong, K.-D. Min, B.-U. Nam, O.O. Park, *Green Chem.*, 18 (2016) 5142.
- [4] N. Jürgensen, J. Zimmermann, A.J. Morfa, G. Hernandez-Sosa, *Scientific Reports*, 6 (2016).
- [5] A. Kowalski, A. Duda, S. Penczek, *Macromolecules*, 33 (2000) 689.
- [6] (a) W.-L. Kong, Z.-Y. Chai, Z.-X. Wang, *Dalton Trans.*, 43 (2014) 14470; (b) M.J.L. Tschan, J. Guo, S.K. Raman, E. Brulé, T. Roisnel, M.-N. Rager, R. Legay, G. Durieux, B. Rigaud, C.M. Thomas, *Dalton Trans.*, 43 (2014) 4550; (c) M.J. Walton, S.J. Lancaster, J.A. Wright, M.R.J. Elsegood, C. Redshaw, *Dalton Trans.*, 43 (2014) 18001; (d) C.-T. Chen, M.-C. Wang, T.-L. Huang, *Molecules*, 20 (2015) 5313; (e) J. Li, Y. Deng, S. Jie, B.-G. Li, *J. Organomet. Chem.*, 797 (2015) 76; (f) R. Petrus, P. Sobota, *Dalton Trans.*, 42 (2013) 13838.
- [7] (a) K. Devaine-Pressing, J.H. Lehr, M.E. Pratt, L.N. Dawe, A.A. Sarjeant, C.M. Kozak, *Dalton Trans.*, 44 (2015) 12365; (b) Y. Wang, W. Zhao, D. Liu, S. Li, X. Liu, D. Cui, X. Chen, *Organometallics*, 31 (2012) 4182; (c) P.-S. Chen, Y.-C. Liu, C.-H. Lin, B.-T. Ko, *J. Polym. Sci., Part A: Polym. Chem.*, 48 (2010) 3564; (d) S. Range, D.F.J. Piesik, S. Harder, *Eur. J. Inorg. Chem.*, 2008 (2008) 3442.
- [8] (a) Z. Zhong, P.J. Dijkstra, C. Birg, M. Westerhausen, J. Feijen, *Macromolecules*, 34 (2001) 3863; (b) L. Piao, Z. Dai, M. Deng, X. Chen, X. Jing, *Polymer*, 44 (2003) 2025; (c) J.M. Colwell, E. Wentrup-Byrne, G.A. George, F. Schué, *Polym. Int.*, 64 (2015) 654; (d) T.-L. Huang, C.-T. Chen, *Dalton Trans.*, 42 (2013) 9255.
- [9] (a) M.M. Kireenko, E.A. Kuchuk, K.V. Zaitsev, V.A. Tafeenko, Y.F. Oprunenko, A.V. Churakov, E.K. Lermontova, G.S. Zaitseva, S.S. Karlov, *Dalton Trans.*, 44 (2015) 11963; (b) P.

Sumrit, P. Chuawong, T. Nanok, T. Duangthongyou, P. Hormnirun, Dalton Trans., 45 (2016) 9250; (c) P.-H. Liu, F.-J. Chuang, C.-Y. Tu, C.-H. Hu, T.-W. Lin, Y.-T. Wang, C.-H. Lin, A. Datta, J.-H. Huang, Dalton Trans., 42 (2013) 13754; (d) Y. Zhang, A. Gao, Y. Zhang, Z. Xu, W. Yao, Polyhedron, 112 (2016) 27; (e) J. Liu, H. Ma, Dalton Trans., 43 (2014) 9098; (f) C. Kan, J. Ge, H. Ma, Dalton Trans., 45 (2016) 6682.

[10] (a) D. Appavoo, B. Omondi, I.A. Guzei, J.L. van Wyk, O. Zinyemba, J. Darkwa, Polyhedron, 69 (2014) 55; (b) S.H. Ahn, M.K. Chun, E. Kim, J.H. Jeong, S. Nayab, H. Lee, Polyhedron, <http://dx.doi.org/10.1016/j.poly.2017.01.050>.

[11] (a) H.-W. Ou, K.-H. Lo, W.-T. Du, W.-Y. Lu, W.-J. Chuang, B.-H. Huang, H.-Y. Chen, C.-C. Lin, Inorg. Chem., 55 (2016) 1423; (b) F.M. García-Valle, R. Estivill, C. Gallegos, T. Cuenca, M.E.G. Mosquera, V. Taberner, J. Cano, Organometallics, 34 (2015) 477.

[12] (a) A. Otero, A. Lara-Sanchez, J. Fernandez-Baeza, C. Alonso-Moreno, I. Marquez-Segovia, L.F. Sanchez-Barba, J.A. Castro-Osma, A.M. Rodriguez, Dalton Trans., 40 (2011) 4687; (b) H.-M. Sun, H.-R. Li, C.-S. Yao, Y.-M. Yao, H.-T. Sheng, Q. Shen, Chin. J. Chem., 23 (2005) 1541.

[13] E.M. Njogu, B. Omondi, V.O. Nyamori, Inorg. Chim. Acta., 457 (2017) 160.

[14] (a) W.-L. Kong, Z.-X. Wang, Dalton Trans., 43 (2014) 9126; (b) K.A. Gerling, N.M. Rezayee, A.L. Rheingold, D.B. Green, J.M. Fritsch, Dalton Trans., 43 (2014) 16498.

[15] C. Fliedel, V. Rosa, F.M. Alves, A.M. Martins, T. Aviles, S. Dagorne, Dalton Trans., 44 (2015) 12376.

[16] (a) M. Mandal, D. Chakraborty, V. Ramkumar, RSC Advances, 5 (2015) 28536; (b) A. Pilone, N. De Maio, K. Press, V. Venditto, D. Pappalardo, M. Mazzeo, C. Pellicchia, M. Kol, M. Lamberti, Dalton Trans., 44 (2015) 2157; (c) N. Nomura, R. Ishii, M. Akakura, K. Aoi, J. Am. Chem. Soc., 124 (2002) 5938; (d) M. Wisniewski, A.L. Borgne, N. Spassky, Macromol. Chem. Phys., 198 (1997) 1227; (e) N. Spassky, M. Wisniewski, C. Pluta, A. Le Borgne, Macromol. Chem. Phys., 197 (1996) 2627.

[17] Bruker, APEXII, in, APEXII Bruker AXS Inc, Madison, Wisconsin, USA, 2009.

[18] Bruker, SAINT, SAINT Bruker AXS Inc, Madison, Wisconsin, USA, 2009.

[19] Bruker, SADABS, Bruker SADABS Bruker AXS Inc, Madison, Wisconsin, USA, 2009.

[20] G. Sheldrick, Acta Crystallogr Sect. A: Found. Crystallogr., 64 (2008) 112.

[21] B. Dolomanov O. V, L. J. Gildea, R. J. Howard, J. A. K. Puschmann, H, Appl. Crystallogr, 42 (2009) 339.

[22] M.L. Cole, G.B. Deacon, C.M. Forsyth, K. Konstas, P.C. Junk, Dalton Trans., (2006) 3360.

[23] M. Cibian, S. Derossi, G.S. Hanan, Dalton Trans., 40 (2011) 1038.

- [24] (a) M. Cibian, S. Langis-Barsetti, J.G. Ferreira, G.S. Hanan, *Eur. J. Inorg. Chem.*, 2016 (2016) 177; (b) M. Cibian, S. Langis-Barsetti, F.G. De Mendonça, S. Touaibia, S. Derossi, D. Spasyuk, G.S. Hanan, *Eur. J. Inorg. Chem.*, 2015 (2015) 73.
- [25] R. Murakami, T. Ishida, S. Yoshii, H. Nojiri, *Dalton Trans.*, 42 (2013) 13968.
- [26] A. Okazawa, Y. Nagaichi, T. Nogami, T. Ishida, *Inorg. Chem.*, 47 (2008) 8859.
- [27] A. Okazawa, D. Hashizume, T. Ishida, *J. Am. Chem. Soc.*, 132 (2010) 11516.
- [28] (a) H.-C. Tseng, M.Y. Chiang, W.-Y. Lu, Y.-J. Chen, C.-J. Lian, Y.-H. Chen, H.-Y. Tsai, Y.-C. Lai, H.-Y. Chen, *Dalton Trans.*, 44 (2015) 11763; (b) N. Buis, S.A. French, G.D. Ruggiero, B. Stengel, A.A.D. Tulloch, I.H. Williams, *J. Chem. Theory Comput.*, 3 (2007) 146.
- [29] R.F. Storey, J.W. Sherman, *Macromolecules*, 35 (2002) 1504.
- [30] T.J.J. Whitehorne, F. Schaper, *Inorg. Chem.*, 52 (2013) 13612.
- [31] E.D. Akpan, S.O. Ojwach, B. Omondi, V.O. Nyamori, *New J. Chem.*, 40 (2016) 3499.
- [32] J.A. Castro-Osma, C. Alonso-Moreno, I. Márquez-Segovia, A. Otero, A. Lara-Sánchez, J. Fernández-Baeza, A.M. Rodríguez, L.F. Sánchez-Barba, J.C. García-Martínez, *Dalton Trans.*, 42 (2013) 9325.
- [33] M. Zikode, S.O. Ojwach, M.P. Akerman, *J. Mol. Catal. A: Chem.*, 413 (2016) 24.
- [34] (a) P. Dubois, C. Jacobs, R. Jerome, P. Teyssie, *Macromolecules*, 24 (1991) 2266; (b) Y. Huang, W. Wang, C.-C. Lin, M.P. Blake, L. Clark, A.D. Schwarz, P. Mountford, *Dalton Trans.*, 42 (2013) 9313.
- [35] E.D. Akpan, S.O. Ojwach, B. Omondi, V.O. Nyamori, *Polyhedron*, 110 (2016) 63.
- [36] L.E.N. Allan, G.G. Briand, A. Decken, J.D. Marks, M.P. Shaver, R.G. Wareham, *J. Organomet. Chem.*, 736 (2013) 55.
- [37] C.-H. Wang, C.-Y. Li, B.-H. Huang, C.-C. Lin, B.-T. Ko, *Dalton Trans.*, 42 (2013) 10875.
- [38] C. Obuah, Y. Lochee, J.H.L. Jordaan, D.P. Otto, T. Nyokong, J. Darkwa, *Polyhedron*, 90 (2015) 154.
- [39] Y.-C. Liu, B.-T. Ko, C.-C. Lin, *Macromolecules*, 34 (2001) 6196.
- [40] M. Bero, B. Czapla, P. Dobrzyński, H. Janeczek, J. Kasperczyk, *Macromol. Chem. Phys.*, 200 (1999) 911.
- [41] N. Spassky, V. Simic, M.S. Montaudo, L.G. Hubert-Pfalzgraf, *Macromol. Chem. Phys.*, 201 (2000) 2432.
- [42] Y. Shen, Z. Shen, Y. Zhang, K. Yao, *Macromolecules*, 29 (1996) 8289.

[43] (a) F. Peng, Z. Shen, *J. Appl. Polym. Sci.*, 106 (2007) 1828; (b) M.P.F. Pepels, P. Souljé, R. Peters, R. Duchateau, *Macromolecules*, 47 (2014) 5542.

[44] (a) A. Rai, S. Senapati, S.K. Saraf, P. Maiti, *J. Mater. Chem. B.*, 4 (2016) 5151; (b) Z. Zhang, X. Chen, X. Gao, X. Yao, L. Chen, C. He, X. Chen, *RSC Advances*, 5 (2015) 18593.

[45] (a) J. Liu, J. Ling, X. Li, Z. Shen, *J. Mol. Catal. A: Chem.*, 300 (2009) 59; (b) E.E. Marlier, J.A. Macaranas, D.J. Marell, C.R. Dunbar, M.A. Johnson, Y. DePorre, M.O. Miranda, B.D. Neisen, C.J. Cramer, M.A. Hillmyer, W.B. Tolman, *ACS Catalysis*, 6 (2016) 1215; (c) N. Ajellal, J.-F. Carpentier, C. Guillaume, S.M. Guillaume, M. Helou, V. Poirier, Y. Sarazin, A. Trifonov, *Dalton Trans.*, 39 (2010) 8363.

[46] (a) D. Li, Y. Peng, C. Geng, K. Liu, D. Kong, *Dalton Trans.*, 42 (2013) 11295; (b) T.-L. Yu, C.-C. Wu, C.-C. Chen, B.-H. Huang, J. Wu, C.-C. Lin, *Polymer*, 46 (2005) 5909.

[47] C. Thomas, B. Bibal, *Green Chem.*, 16 (2014) 1687.

Graphical abstract

Mononuclear Zn(II) and Cu(II) *N*-hydroxy-*N,N'*-bis(2,6-diisopropylphenyl)formamidine complexes were synthesized. Structural studies showed that the metal center in Zn(II) complexes prefer a distorted tetrahedral geometry and square planar for Cu(II) complexes. In both complexes, the coordination sites are occupied by imino *N* and hydroxyl *O* donor atoms from the chelating ligand. They displayed catalytic activity in ring-opening polymerization of ϵ -caprolactone and *L*-lactide in the presence of a co-initiator furnishing low molecular weight polymers

